CHAPTER 18

MAGNETOSTRICTIVE MATERIALS

Most of the magnetoelastic effects described in chapter 12 have industrial applications: controlled thermal expansion alloys, actuators and sensors. In this chapter we present the most widely used magnetostrictive materials as well as their principal industrial applications.

1. THE INVAR AND ELINVAR FAMILY

1.1. CONTROLLED THERMAL EXPANSION ALLOYS

In fabricating complex mechanical assemblies for use under extreme temperature conditions, one has to consider the compatibility of the thermal expansion of the various components. Typical examples include cryogenic liquid containers, the inner and outer walls of which are at very different temperatures, and metallic pieces soldered to materials with low thermal expansion coefficients (e.g. metal-glass solder). Exploiting the strong positive volume magnetostriction of certain iron alloys, metallurgists have developed a whole family of alloys with tuneable thermal expansion, i.e. the thermal expansion coefficients of which can have values much lower than those of classic alloys.

The archetype of these alloys is *Invar®,* of composition $Fe_{65}Ni_{35}$, discovered in 1896 by C.E. Guillaume, which shows practically zero thermal expansion at room temperature. Some characteristics of three Invar-type alloys, commercially developed by Imphy SA, are shown in table 18.1.

Invar is used when a material with very low thermal expansion at ambient or low temperatures is needed. The applications of Invar are very diverse, ranging from enormous methane tankers to tiny parts for metrology, and including such applications as high definition colour TV masks.

The remarkable physical properties of this alloy are related to the extreme sensitivity of its electronic structure to interatomic distances. The iron atoms have the remarkable property, in the face centred cubic alloy, of existing in two different spin states: one spin state conforms to Hund's rules, and gives rise to a high value of magnetic

moment (2.2 to 2.5 μ_B) and to a larger crystalline cell parameter while the other spin state gives rise to a smaller magnetic moment (0.8 to 1.5 μ_B) and a smaller cell parameter.

Table 18.1 - Principal physical characteristics of crystallised alloys with tuned thermal expansion (Imphy Ugine Précision)

Properties	Invar	Dilver 0	Dilver P_0
α_T, 10^{-6} K^{-1}	1[a], 0.6[b], 1.9[c], 4.7[d]	8.9[a], 9.8[c], 10.6[e], 11.4[f]	6.5[a], 5.5[c], 4.9[e], 7.5[f]
Specific mass, $kg.m^{-3}$	8130	7500	8250
Tensile stress, MPa	600	800	730
(" after anneal)	(500)	(570)	(550)
Vickers hardness	200	230	220
(" after anneal)	(130)	(180)	(150)
Melting temperature, K	1723	1723	1723
Thermal conductivity, $W.m^{-1}.K^{-1}$	10.5	12.1	17.5
Specific heat, $J.K^{-1}.kg^{-1}$	510	500	500
Electrical resistivity, $\mu\Omega.m$	0.75	0.65	0.49
Curie temperature, K	503	843	698
Magnetic polarization, T	1.6	–	1.6

α_T is measured between −100 and 0°C [a], 0-100°C [b], 100-200°C [c], 200-300°C [d], 300-400°C [e], 500-600°C [f].
The other properties are measured at room temperature.

When heating these alloys from low temperature, we progressively populate the second state, and the resulting cell contraction roughly compensates the normal thermal expansion: in figure 18.1 we see that the volume of the alloy is almost invariable between 0 and about 400 K, an observation which gave rise to the name Invar, a registered trademark of Imphy Ugine Précision.

The Invar effect is an exchange magnetostriction effect but it is the value of the atomic magnetic moment, more so than the exchange integral, which changes with distance.

The Invar alloy is still the reference alloy in this domain, but many other families of alloys showing similar properties have been since discovered. These new alloys are special steels with *tuneable thermal expansion,* and have an ever growing number of applications: metrology, high resolution television, metal-glass solder, methane tankers, etc. [1].

These alloys possess a giant volume magnetostriction, and consequently a forced magnetostriction which is about 50 times greater than that of other ferromagnetic substances ($\partial V / V \partial H = 1.2 \times 10^{-10} / A.m^{-1}$), which can cause problems: to secure perfect dimensional stability, the invar must be shielded from all magnetic fields or else replaced by an antiferromagnetic alloy which, to a first approximation, is

insensitive to magnetic fields. However, antiferromagnetic substances with a linear thermal expansion coefficient of less than $4 \times 10^{-6}\ K^{-1}$ have not yet been discovered.

The temperature dependence of the linear thermal expansion coefficient α_T of the $Fe_{65}Ni_{35}$ Invar alloy is compared with that of Ni in figure 18.1: while anomalies occur for both Ni (representative of "normal" magnetic metals and alloys) and Invar at around T_C, an additional anomaly occurs at lower temperature in the Invar. Note the dramatic reduction in α_T below the T_C of Invar: however the thermal expansion coefficient is close to zero just near 100 K and 290 K.

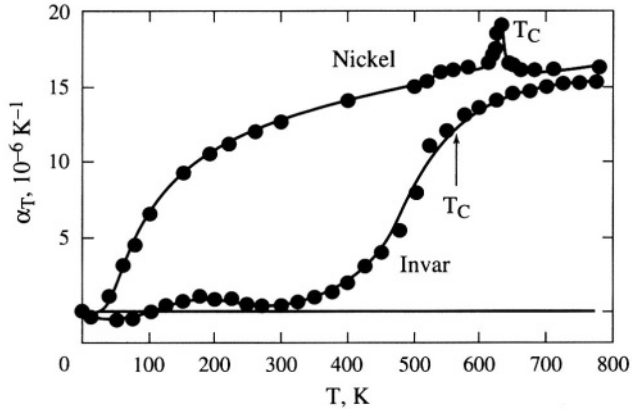

Figure 18.1 - Temperature dependence of the linear thermal expansion coefficient of Invar, *after [2],* ***and nickel,*** *after [3]*

The Dilvers are used for fracture-free glass-metal soldering in electronic assemblies submitted to significant thermal variations above room temperature.

Certain Fe based amorphous alloys have thermal expansion coefficients which also remain low due to their strong positive volume magnetostriction: e.g. ribbons of Metglas® 2605SC have a linear thermal expansion coefficient $\alpha_T = 5.9 \times 10^{-6}\ K^{-1}$, which is half that of Co based Metglas® 2705M. This weak expansibility occurs together with remarkable mechanical and magnetic properties, as can be seen in table 18.2.

1.2. ALLOYS WITH CONSTANT ELASTIC MODULI

Giant second order magnetoelastic effects were also observed in the family of Invar alloys, again by C.E. Guillaume, the discoverer of Invar and a Nobel Laureate for physics. In 1920 he discovered **Elinvar,** an alloy of Fe containing 36% nickel and 12% chromium, which has a face centred cubic structure leading to a Young's modulus which does not vary with temperature: in this case it is the magnetic contribution to the elastic constant which compensates the normal thermal variation of this constant. A number of alloys exhibit this "Elinvar effect".

Such alloys are industrially interesting and can be used in precision engineering, e.g. in watchmaking technology, to make springs the stiffness of which remains unaffected by thermal variations [1].

For applications, the objective is not always to have thermal invariance of Young's modulus, $\partial Y / \partial T = 0$. The aim can be the invariance of the specific property exploited in a given application.

For example, if we use the mechanical resonance frequency of a bar of length ℓ in a longitudinal vibration mode $f_0 = (1/2\ell)(Y/\rho)^{1/2}$, it would be convenient to make f_0 independent of temperature. This leads to: $\partial \ln(Y)/\partial T = -\partial \ln(\ell)/\partial T$, since the specific mass ρ varies as ℓ^{-3}. In general, Young's modulus Y decreases as temperature increases while ℓ increases: the two effects can thus compensate, leading to the thermal stability of f_0.

2. MAGNETOSTRICTIVE MATERIALS FOR ACTUATORS

2.1. MATERIALS WITH HIGH ANISOTROPIC MAGNETOSTRICTION

Materials with a high anisotropic magnetostriction (Joule magnetostriction) are sought to make all sorts of actuators. They must produce relatively large deformations in the smallest excitation fields possible. As magnetostriction is an even effect with respect to magnetization, it is necessary to polarise the material with a static magnetic field so as to operate near the inflection point of the $\lambda(H)$ characteristic, called the *average working point.*

We recall that the coefficients s_{ij}^H, μ_{kl}^σ and d_{mn}, defined (see eq. 12.41) around this working point, may be functions of the applied field and depend on the previous history of the material. Values found in literature are then average values.

Characteristic data of diverse magnetostrictive materials are compared in table 18.2. k_{33} and d_{33} are defined in § 9.1 of chapter 12.

We see that certain rare earth based alloys discovered around 75 (in grey in tab. 18.2) show magnetostrictive deformations 50 to 100 greater than those of conventional materials discovered in the 1950's and 1960's (nickel and alfer); we will now see why and how.

2.2. TERFENOL-D

This alloy deserves particular attention for two reasons: firstly, it is the best candidate for a room temperature magnetostrictive actuator (in 1990 it set the world record for sonar acoustic power density); secondly, it is the product of model research in the domain of magnetic materials.

Table 18.2 - Curie temperature, and room temperature physical properties of some magnetostrictive materials

Substance	T_C (K)	J_s (T)	λ_s (10^{-6})	ρ_e (μΩm)	k_{33}^{max}	d_{33}^{max} (mA^{-1})
Nickel	631	0.63	–36	0.07	0.31	-3.1×10^{-9}
Alfer (Fe 13%Al)	773	1.3	+40	0.9	0.32	7.1×10^{-9}
45 Permalloy (Fe 65%Ni)	713	1.6	+27	0.6	0.17	–
2V-Permendur (2V, 49Fe, 49Co)	1,253	2.4	+70	0.3	0.26	–
Ni 4%Co	683	0.68	–31	0.1	0.50	–
Magnetite (Fe_3O_4)	853	0.61	+40	10^2	0.36	–
Nickel Ferrite ($NiFe_2O_4$)	863	0.33	–33	$>10^{10}$	0.20	–
$Ni_{0.98}Co_{0.02}Fe_2O_4$	863	0.33	–32	$>10^{10}$	0.38	–
DyZn [001] at 4.2 K	140	anisotr.	(+5,300)	0.5	–	–
Terfenol ($TbFe_2$)	698	1.1	+1,750	–	0.35	–
Terfenol-D* ($Tb_{0.3}Dy_{0.7}Fe_2$)	653	1.0	+1,100	0.6	0.75	57×10^{-9}

* *Note that d_{33} is very sensitive to stress for Terfenol-D (57×10^{-9} m.A^{-1} under 0 MPa, but only 10×10^{-9} m.A^{-1} under 40 MPa).*

Originally, engineers charged with designing magnetostrictive actuators were interested in two classes of materials:

- 3d metals and alloys which are capable of working at room temperature, and under relatively low magnetic fields, but have too weak a magnetostriction to compete with piezo-electric ceramics,
- 4f metals which show giant magnetostrictions, but very low Curie temperatures, complex magnetic structures, and such high magnetocrystalline anisotropies that large magnetic fields would be required to produce noticeable deformation.

It appeared that it might be possible to obtain materials with high magnetostriction even at room temperature, and under reasonable excitation, by alloying rare earths with 3d metals such as iron and/or cobalt.

A.E. Clark discovered the alloy $TbFe_2$, also known as *Terfenol* (**Ter**bium, **Fe, N**aval **O**rdnance **L**aboratory), which combines a relatively high Curie temperature due to the iron and a giant magnetostriction due to the terbium. However, this alloy's high magnetocrystalline anisotropy limits its use. Soon after, in 1975, Clark prepared a new alloy $Tb_{0.3}Dy_{0.7}Fe_2$, known as *Terfenol-D* (D for **D**ysprosium), which maintains a giant magnetostriction and a relatively high Curie temperature, but which can be saturated in moderate magnetic fields. Saturation is possible for this composition because, to first order, the contributions of terbium and dysprosium to the magneto-crystalline anisotropy cancel at room temperature. We note the strong anisotropy of its magnetostriction: $\lambda^{\varepsilon,2}$ is 2.4×10^{-3}, while $\lambda^{\gamma,2}$ is at least one hundred times weaker.

From equation (12.21), that is: $\lambda_s = (4/15)\lambda^{\gamma,2} + (2/5)\lambda^{\varepsilon,2}$, we see that an *isotropic* polycrystalline Terfenol-D sample will attain just 40% of $\lambda^{\varepsilon,2}$. It thus seems preferable to prepare textured samples, favouring the [111] direction if possible. This has proved difficult, and samples used on an industrial scale have, up to recently, been textured bars with orientation $[11\bar{2}]$. Two techniques have been developed to prepare samples: the modified Bridgman (MB) technique, and the "Free Standing Zone" or FSZM technique. Both techniques produce twinned bicrystals with the $[11\bar{2}]$ direction in the twin plane, which produces significant internal stress at the twin boundary, and somewhat reduces the d_{33} coefficient of magnetostrictivity. The maximum deformation $\Delta\lambda = (1/6)\lambda^{\gamma,2} + (5/6)\lambda^{\varepsilon,2}$ expected for such a texture is of the order of 2×10^{-3}. Much effort is being made to improve the performance of this alloy and to reduce its fabrication cost: [111] oriented bars have been prepared in China by the Czochralski method in a cold crucible and in levitation [4], and more recently the Japanese company TDK brought to the market bars produced from a powder route which show significant magnetostrictivity in weak fields [5].

Due to their texture, there is some confusion about the definition of *magnetostriction coefficients* for materials with "giant magnetostriction". λ_s is by definition the coefficient measured on a non-textured polycrystalline sample, given by equation (12.21) cited above.

In fact, manufacturers often give as the "magnetostriction coefficient" the value $\lambda_{//}$ of the longitudinal magnetostriction measured in the $[11\bar{2}]$ direction in a pre-stressed grain oriented sample, which is markedly higher than the value of λ_s. Finally, dynamic deformation under resonance conditions can greatly overcome the theoretical static limit, as we saw in § 9.3 of chapter 12: a dynamic deformation of 3.5×10^{-3} was observed under resonance for Terfenol-D, although λ_s is only 1×10^{-3}.

It is the high energy density of Terfenol-D which allows it to compete with ceramic piezo-electrics. It is instructive to compare the relative displacement of the ends of bar-shaped samples of laminated ceramic PZT and Terfenol-D as a function of the pressure applied by the actuator (fig. 18.2).

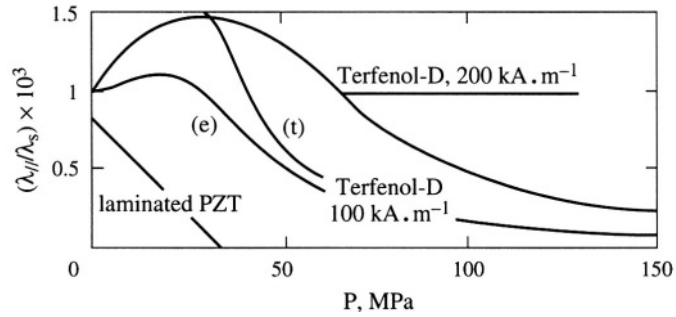

Figure 18.2
Comparison of the reduced deformation of two identically shaped bars of Terfenol-D, and laminated ceramic PZT, as a function of the applied pressure P

The available energy is given by the area under the curve: thus the Terfenol-D compares favourably as shown for the experimental curves at H = 100 and 200 $kA.m^{-1}$. The theoretical curve (t), given for $H = 100\ kA.m^{-1}$, is calculated in exercise 3 *neglecting magnetocrystalline anisotropy,* which explains why it does not describe correctly the behavior at low stress (theory predicts that all compressive stresses less than 35 MPa increase $\lambda_{//}$ from λ_s to $(3/2)\lambda_s$ but experiment shows that a field of at least $200\ kA.m^{-1}$ must be applied if $\lambda_{//}$ is to approach such a value).

Until recently, at least eight companies had commercialised Terfenol-D: two in Europe, Johnson & Matthey - Rare Earth Products in Great Britain, and Feredyn Europe in Sweden which have since ceased production, two in the USA, Etrema Products (subsidiary of Edge Technologies), and EDO, the most important producer of piezoelectric ceramis, and four in Japan, TDK, NKK, Toshiba and Sumitomo. The standard products are cylindrical bars, tubes and disks. The properties vary slightly according to the preparation technique used, the sample's history and the operating conditions. Some average physical properties of products supplied by three producers are given in table 18.3.

Table 18.3 - Physical properties of Terfenol-D alloys at 20°C

Properties	Units	Etrema a	Reacton Magmek b	Magmek 86 c	Magmek 91 c
Specific mass (ρ)	$kg.m^{-3}$	9,250	9,250	9,100	7,300
Linear thermal expansion coefficient (α_T)	$10^{-6}\ K^{-1}$	12	12	12	
Compressibility modulus (κ)	GPa	90			
Young's modulus (Y^H)	GPa	25-35		26.5[d]	22[d]
Young's modulus (Y^B)	GPa		50	55	
Velocity of sound (v^H)	$m.s^{-1}$	1,720		1,720[d]	1,740
Velocity of sound (v^B)	$m.s^{-1}$		2,450	2,450	
Compressive strength	MPa	700		300	250
Tensile strength	MPa	28		28	120
Specific heat (C_p)	$J.K^{-1}.kg^{-1}$	320-370			
Thermal conductivity	$W.m^{-1}.K^{-1}$	10.5			
Electrical resistivity (ρ_e)	$\mu\Omega.m$	0.6	0.6	0.6	10^4
Curie temperature (T_C)	K	653		660	
Magnetic polarization ($\mu_0 M_s$)	T	1			
Relative permeability (μ_{33}^{τ}/μ_0)	–	5 - 10	10	9.3	2 - 12
Relative permeability ($\mu_{33}^{\varepsilon}/\mu_0$) [e]	–			4.5	
Joule magnetostriction ($\lambda_{//}$)	10^{-3}	1.5 - 2	1.5	1.4 - 1.8	1.1
Magnetomechanical coupling (k_{33}^{max})	–	0.7 - 0.8	0.5 - 0.8	0.72	
Static magnetostrictivity (d_{33}^{max})	$nm.A^{-1}$	24[f] 57[g]	12	17	4
Dynamic magnetostrictivity (d_{33}^{max})	$nm.A^{-1}$		6[h]		
Elastic energy density	$kJ.m^{-3}$	14 - 25		14 - 25	11

[a] Etrema Products-Edge (USA) [b] Johnson-Matthey (UK) [c] Feredyn AB (Sweden) [d] Demagnetised state [e] $\mu_{33}^{\varepsilon}/\mu_0 = \mu_{33}^{\tau}(1 - k_{33}^2)/\mu_0$ [f] MB alloy [g] FSZM [h] alloy under 45 GPa.

We note that the electrical resistivity of Terfenol-D is in general weak, except for the Magmek-91 composite which is specially prepared for high frequency applications. This composite also possesses a much higher tensile strength (120 MPa compared to 28 MPa), but these improved characteristics are achieved at the cost of a loss of magnetostrictivity ($d_{33} = 4\ nm.A^{-1}$ instead of 10 to $60\ nm.A^{-1}$). Finally we note that the prototype [111]-oriented single crystal bars produced in China [4] have an even higher magnetostriction reaching $75\ nm.A^{-1}$.

Research into terfenol alloys remains active, and it is probable that a greater range of transducer bars will be available in the future. The coefficient of magnetomechanical coupling k_{33}^{max}, which is an important parameter, now reaches values of 0.75, which is much higher than values achieved in the past.

It must be remembered that the parameters quoted in table 18.3 correspond to the optimum values recorded at 20°C; the magnetostrictivity decreases rapidly as we move away from this temperature, and also if we pre-stress the transducers, a treatment which is generally desired due to their fragility.

Figure 18.3 shows the thermal variation of the magnetostriction of a bar of Terfenol-D submitted to a compressive stress of 19 MPa: in weak fields, from 20 to $40\ kA.m^{-1}$, the magnetostriction remains almost constant between 0°C and 90°C, but this is not the case in higher fields [6].

The compensation between the positive magnetocrystalline anisotropy of dysprosium and the negative magnetocrystalline anisotropy of terbium is perfect at only one given temperature, which explains why the performance of this alloy is strongly reduced away from this optimum temperature. Nevertheless, the exceptional qualities of these materials justify their use despite the need for crude temperature regulation.

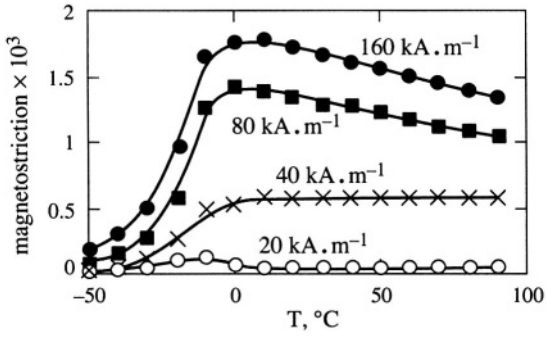

Figure 18.3 - Thermal variation of the magnetostriction of Terfenol-D

These curves, which are very sensitive to stress, were measured on bars submitted to a pre-stress of 19 MPa.

Too high an excitation frequency can also degrade the above quasi-static performance. Due to the skin effect related to eddy current losses, the dynamic magnetostrictive characteristics, such as the apparent magnetomechanical coupling coefficient, may

depend on the shape of the active element if the frequency becomes higher than a characteristic frequency f_c, which, for a cylinder of diameter d and electrical conductivity γ, is given by:

$$f_c = 2/(\gamma \pi \mu_{33}^{\varepsilon} d^2) \qquad (18.1)$$

where μ_{33}^{ε} is the magnetic permeability at constant deformation. The use of a composite of low electrical resistivity is then recommended.

In conclusion, at room temperature, Terfenol-D is comparable with ceramic PZT because of its strong saturation deformation and its high power density. Moreover, for low frequency applications, the lower velocity of sound (2,450 $m.s^{-1}$ for Terfenol-D compared to 3,100 $m.s^{-1}$ for PZT) allows resonance to be achieved with shorter bars. It is also better than electrostrictive materials such as PMN-PT, the good performance of which disappears at 40°C (their Curie temperature).

The principal disadvantages of Terfenol-D seem to be its hysteresis, a relative sensitivity to temperature, the necessity of magnetically polarising them and their high cost; finally we mention the fragility of the stoichiometric alloy under traction. The remedy is to hold the samples under compression and to remain slightly under-stoichiometric in iron: this is why the composition of alloys available on the market is $Tb_{0.3}Dy_{0.7}Fe_x$ with x varying from 1.90 to 1.95 without a great variation in magnetostrictive performance.

2.3. USE OF TERFENOL-D IN ACTUATORS

Owing to their strong magnetostriction, Terfenol-D alloys are able to produce significant force, and generate rapid, precise movement with considerable power. The main industrial applications of Terfenol-D are linear actuators, which in essence are magnetostrictive bars, polarised by a static magnetic field, and usually submitted to a compressive stress, which elongate under the influence of a quasi-static or dynamic excitation field.

Some concrete examples will illustrate the precautions to be taken in selecting the most appropriate material for a given application: electro-valves (fuel injection, cryogenic applications…), micro-pumps (heads of ink jet printers), automatic tool positioning with wear compensation (machine tools), active vibration damping, fast relays, gears, auto-locking actuators (robotics), rapid shutters, automatic focusing (optics), hooping under field (when a bar of Terfenol-D elongates, its diameter decreases). More detailed information can be obtained in a recently published reference book [7].

2.3.1. Linear actuator

An example of a linear actuator is shown in figure 18.4. We see here how much the magnetic and mechanical aspects intimately overlap: it is thus best to design the entire system so as to optimise performance. Software has been developed for this purpose.

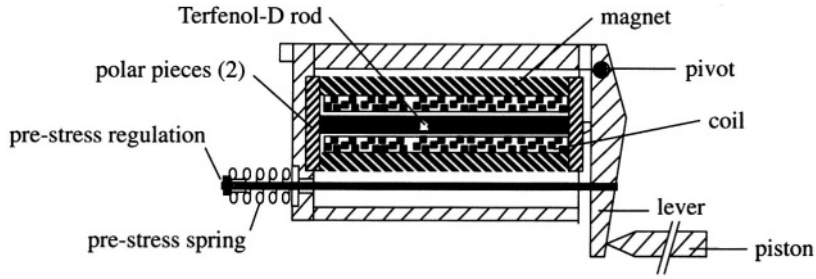

Figure 18.4 - An example of a linear actuator
(Documentation Etrema Products, Ames, IA, USA)

2.3.2. Differential actuator

Another prototype, the differential actuator, deserves to be mentioned because starting from two rectilinear movements, it can produce rotational motion of the mobile axis (fig. 18.5).

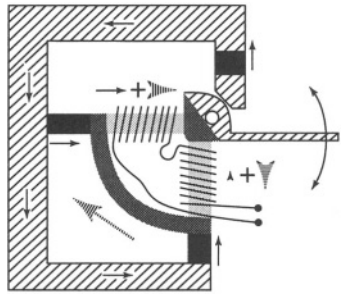

Figure 18.5 - Differential actuator

Static flux is shown by black arrows, dynamic flux by the hashed arrows. Soft magnetic material: hashed volumes; Terfenol-D bar: in light grey (under coils); magnets: in black; insulating soft magnetic materials: in dark grey[8].

Nevertheless, the motion is very restricted. The static (polarization) and dynamic (excitation) magnetic fluxes follow different paths, so it is possible to observe, in two bars placed at right angles, a dynamic magnetic field which reinforces the static field for one bar and opposes the magnetic field for the other. Thus, the first bar elongates while the second shortens, which generates the desired rotational motion.

To allow magnetostrictive bars to remain permanently under stress, it is also possible to use two aligned bars which work symmetrically: when the first elongates, the second shortens. This “push-pull” assembly is particularly well adapted to active position control since, after expansion, one of the two elements is always returned to its contracted position by the other which then expands.

2.3.3. Wiedemann effect actuators

Another very particular type of actuator exploits the direct Wiedemann effect: it consists of a spiral spring made from a magnetostrictive wire which is coated by a winding which allows it to be longitudinally magnetised.

When a current circulates in the spring, the latter is submitted to a helical magnetic field (see § 5 of chapter 12), and experiences a twisting due to the Wiedemann effect,

which generates a linear displacement of one end of the spring if the other end remains fixed (fig. 18.6). Such an actuator was designed and actually used as a micropositioner of heavy optical pieces in a telescope.

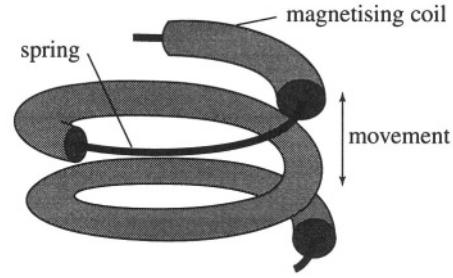

Figure 18.6
Wiedemann effect actuator [9]

2.3.4. Magnetostrictive linear motor

This motor consists of just a bar of Terfenol-D and a tube of the same diameter, which acts as the stator: as Joule magnetostriction develops at constant volume, it is possible to move the bar up and down the tube by applying a magnetic field, and then to block the bar in a given position by suppressing the magnetic field. What is happening is that as the bar elongates its diameter decreases under the magnetic field, and then increases again when the field is suppressed. This explains the total absence of backlash in this type of motor designed by L. Kiesewetter in Berlin: the mobile part is blocked in the absence of exciting currents. The movement is thus generated by a magnetic field applied along a small length starting at one end of the bar: the diameter decreases and the length of bar which experiences the field is free to elongate. As the field is moved to the other extremity of the bar, the deformed zone also moves, and finally, when the magnetic field is suppressed, the bar regains its initial length but has been displaced by a distance h in the direction opposite to that in which the field was moved, as shown in figure 18.7.

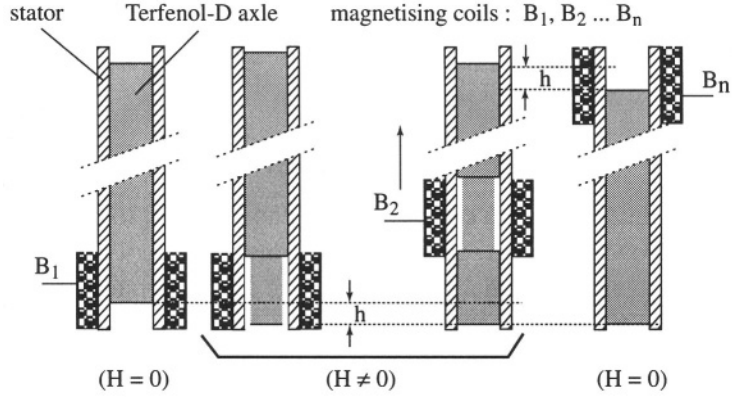

Figure 18.7 - Kiesewetter's linear magnetostrictive motor

The axle, made of Terfenol-D, advances like a caterpillar, by crawling.
It can support very heavy loads, even when stationary [10].

Repeating the cycle several times, we have a linear stepper motor. Reverse motion is produced by applying the field in the opposite direction. In practice, the field is created successively by n coils B_1, B_2, B_n, placed side by side. For a 10 cm long bar of magnetostriction 10^{-3}, a displacement of $10\ \mu m$ can be produced by exciting ten 1 cm segments successively. With 10 cycles per second, the bar is moved with a velocity of 0.1 mm per second. The length of the run is limited by the geometry of the device, more specifically by the length of the stator. The maximum admissible load depends on the mechanical performance of the stator: e.g. such a motor could be used to position loads of more than a ton with a 1 micron precision (see exercise 4 at the end of the chapter).

2.3.5. Magnetostrictive rotary motors

It is possible to create rotary stepper motors by combining two out of phase linear movements according to the principles of friction motors or four stroke electric motors. Most of these motors have two essential characteristics in common, a very *strong torque* (even at zero velocity), and a *total absence of backlash.*

Friction motors comprise two perpendicular linear actuators. One can put the stator in contact with a rotor, and when the contact is made, the second actuator displaces the rotor. The first actuator then retracts, and the second can return to its rest position without moving the rotor. Actually, the two movements are simultaneous, and the point of contact of the stator describes an ellipse. A motor torque of 2 Nm has already been achieved with such a motor. Significant progress is still expected, but the main drawback of this type of motor is the friction wear of the surfaces in contact, as in the case of piezoelectric motors.

The four stroke rotary electric motor works in a different way:
1. actuators grip the rotor,
2. then they are pushed by a second assembly of actuators,
3. the grip of the first actuator is released, freeing the rotor,
4. and the second assembly of actuators return to their rest position.

The motor is then ready for a new cycle. A 1991 prototype was able to produce a torque of 12.2 Nm on the rotor [11].

Mixed motors, which use magnetostrictive and piezo-electric materials at the same time, have also been constructed. The mechanical performances of these two classes of materials are very different and may be complementary, in particular in the domain of shear resistance.

In conclusion, we expect strong torques, even at low speeds, for magnetostrictive motors. At zero velocity the motor maintains its position without the least bit of backlash. Comparison with piezo-electric motors is not easy because of the extensive research being carried out in both domains. However, we can predict that magnetostrictive motors, because of their higher costs, will be reserved for high energy density applications, e.g. aerospace devices.

Specific power ratings for the major motor types of the 1990's are of the order of $20\ W.kg^{-1}$ for a standard electric motor, $50\ W.kg^{-1}$ for a servo-motor, $80\ W.kg^{-1}$ for a piezo-electric based ultrasonic motor, and $100\ W.kg^{-1}$ for a magnetostrictive motor. The comparison of such different devices is not easy, as it should also take account of the weight and bulkiness of the energy sources used.

2.3.6. Sonar

The transmission of electromagnetic waves in salty ocean water encounters such attenuation that it is impossible to imagine guiding or locating an obstacle with the aid of radar. Thus, in 1935 submarines started using the sonar technique which involves emitting acoustic waves and measuring the time it takes the echoes to return to deduce the distance from a reflecting object. At first nickel was used, as it could act as the emitter, due to Joule magnetostriction, and at the same time as the receiver, due to the inverse effect. When nickel became scarce during the war, it was replaced by an aluminium iron alloy named "Alfenol" or "Alfer". After the second world war, magnetostrictive materials were replaced by ceramic piezo-electrics. Today, there is renewed interest in the use of magnetostrictive devices, and prototypes made with Terfenol-D have broken the world record for emitted power density.

Emitters usually consist of pre-stressed bars, with one extremity connected to an impedance adapter which couples the bar to the sea water. The polarization is induced by permanent magnets [12].

3. SENSOR MATERIALS

Research has been active in the domain of magnetostrictive sensors ever since the discovery of the Wiedemann effect torque-meter by Kobayosi in 1929, and it has experienced an unprecedented expansion with the discovery of Metglas 2605SC. The best materials for magnetostrictive sensors are not those with giant magnetostriction, but those which can convert elastic energy into magnetic energy, or *vice versa,* with an efficiency that approaches 100% so as to minimise signal loss.

This condition thus favours materials with the *highest possible value of the magnetomechanical coupling coefficient and the lowest possible losses.* The parameter to be optimised is not λ_s, but $\partial\lambda/\partial H$, or the magnetostrictivity d_{33}, which also characterises the sensitivity of the material's magnetization to stress. Metallic nickel –although very vulnerable to shock– was used as a sonar detector during the second world war, but was then replaced by piezo-electric ceramics. In the 1980's, a metallic glass with excellent magnetoelastic properties, Metglas® 2605SC, the characteristics of which are given below, appeared as a serious competitor for piezo-electric ceramics.

The magnetostrictivity $\partial\lambda/\partial H$ can be increased by annealing the material. This releases internal stresses and increases the initial magnetic permeability, without necessarily modifying the value of the saturation magnetostriction, λ_s (see fig. 12.15). In the case of amorphous materials, an anneal at temperatures *less than* the recrystallization temperature T_X, can sometimes induce a structural relaxation and thus slightly modify λ_s, while an anneal at a temperature *above* T_X always strongly modifies λ_s, which is sensitive to local atomic order.

Note - *There are experimental circumstances when the above demands do not apply. Realising it can lead to a more economical design. Later we will see how to construct a torque sensor based on the inverse Wiedemann effect. In this device, the sensor contains a magnetic head which is situated some tenths of mm from the shaft to allow torque measurement even when the shaft is rotating: thus, most of the magnetic reluctance is concentrated in the air-gap. Whether the material has a permeability of 10,000 or 300, and whether the magnetomechanical coupling coefficient k is 0.99 or 0.75, the sensor's response curve will be practically the same!*

The solution is to use a shaft made of ordinary steel, and to measure the modulation of its permeability under stress: generally the sensitivity will be sufficient.

3.1. METGLAS 2605SC

Today's best isotropic magnetostrictive material is an iron rich metallic glass, Metglas® 2605SC, produced by *Allied Signal Inc.*. This is the material most suited for making high sensitivity magnetoelastic sensors. It is an $Fe_{81}B_{13.5}Si_{3.5}C_2$ alloy prepared by melt spinning: a stream of molten alloy is projected onto a cold wheel where it is cooled by a thousand degrees in one thousandth of a second. This freezes the alloy in the liquid state (it is amorphous, i.e. non-crystallised). The ribbons have widths of 10 to 100 mm, and a thickness of about $20\ \mu m$.

Table 18.4 contains some properties of this alloy which is frequently used in all sorts of sensors. Its electrical resistivity is 20 times greater than that of nickel, for a comparable magnetostriction which is however positive. Note its very interesting elastic properties, its weak thermal expansion coefficient, and its good corrosion resistance.

Annealing the ribbon in a magnetic field applied in its plane, but perpendicular to the ribbon length, for 10 minutes at 642 K, induces a very weak magnetic anisotropy ($K = 35\ J.m^{-3}$) with the easy direction of magnetization along the direction of the applied field. A longitudinal magnetic field of the order of $50\ A.m^{-1}$ is sufficient to compensate for this weak anisotropy: thus a magnetomechanical coupling coefficient close to 1 is observed ($k_{33} = 0.97$).

Table 18.4 - Physical properties of a Metglas 2605SC ribbon annealed under magnetic field

Properties (symbols)	Units	Annealed Metglas 2605SC
Density (ρ)	$kg.m^{-3}$	7,320
Crystallization temperature (T_x)	K	753
Linear thermal expansion (α_T)	$10^{-6} K^{-1}$	5.9
Young's modulus (Y^H)	GPa	25
Young's modulus (Y^B)	GPa	200
Vickers hardness under 50g (H_v)	–	880
Tensile elastic limit	MPa	700
Thermal conductivity	$W.m^{-1}.K^{-1}$	9
Electrical resistivity (ρ_e)	$\mu\Omega.m$	1.35
Curie temperature (T_C)	K	643
Magnetic polarization ($J_s = \mu_0 M_s$)	T	1.35 ($H = 80 A.m^{-1}$) 1.61 (satn.)
Initial relative permeability (μ_{33}^{τ}/μ_0)	–	20,000 (80,000 at $\sigma_{zz} = 1$ MPa)
Maximum relative permeability (μ^{max})	–	300,000
Magnetostriction coefficient (λ_s)	10^{-6}	30
Magnetomechanical coupling coeff (k_{33}^{max})	–	0.97 ($H = 50 A.m^{-1}$)
Static magnetostrictivity (d_{33}^{max})	$nm.A^{-1}$	1,000

3.2. SENSORS BASED ON INVERSE MAGNETOELASTIC EFFECTS

The inverse Joule magnetoelastic effect (see § 6.2 of chap. 12) is exploited in simple *force, percussion* and *pressure* sensors. The geometry of these sensors can be infinitely varied, but the working principle remains the same: pick-up coils measure the flux variations generated by changes in stress applied to a weakly magnetised Metglas ribbon.

3.2.1. Force sensor

A ribbon of metallic glass, of composition $Co_{75}Si_{15}B_{10}$, which has a negative magnetostriction λ_s, is suspended and maintained vertical by the application of a weak tensile force (fig. 18.8-a). An exciting coil is used to create an AC magnetic field at the centre of this ribbon. Two pick-up coils detect the induced flux variations. The hysteresis loop corresponding to this "free ribbon" situation is shown in figure 18.8-b, where it is compared with the loop measured when a supplementary stress is applied in addition to the initial tensile stress ("loaded ribbon"). The flux variation in the pick-up coils, which is related to the decrease in the permeability of the ribbon, is significant around zero field. Thus such sensors have a very high sensitivity, but are also very sensitive to all variations in excitation current: this is the reason why it is preferable to operate near the "pseudo-saturation" value of induction, B_{max}. This

markedly reduces the sensor's sensitivity to current variations; figure 18.8-c shows the characteristic response of such a sensor.

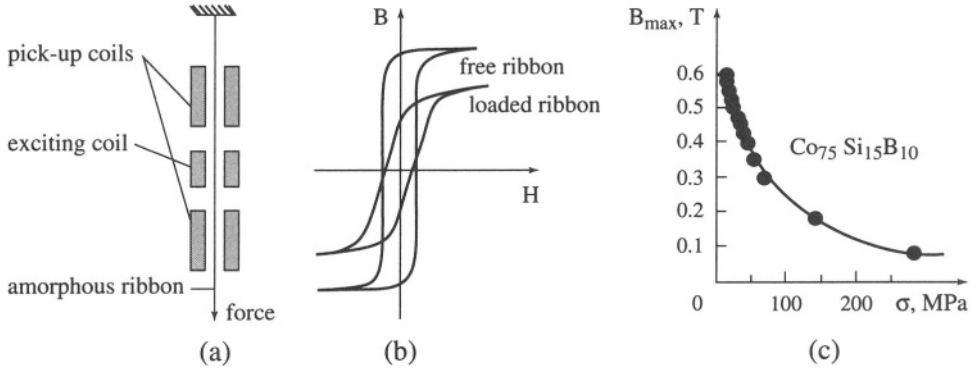

Figure 18.8 - Force sensor in which pick-up coils measure the flux variations generated by changes in applied stress [13]

3.2.2. Ultrasensitive magnetometry

Based on a very different principle, a sensitive magnetometer can be made from a ribbon of Metglas deposited on a piezo-electric ceramic substrate oscillating at resonance; under the effect of this oscillatory stress, the magnetization of the ribbon is modulated with an amplitude proportional to the external magnetic field. When the magnetic field is modulated at a low frequency F, it is possible to detect the AC component by lock-in detection: the ultimate sensitivity of the machine, which varies with frequency $(1/F)^{1/2}$, reaches that of ultrasensitive "flux gate" type magnetometers, i.e. of the order of 10 pT at 1 Hz.

3.2.3. Inverse Wiedemann effect torquemeter

The inverse Wiedemann effect can be exploited to measure, without contact, and from a distance, the torque exerted on a ferromagnetic, and magnetostrictive shaft. Under the influence of the torsion generated by the torque, such a shaft will have an anisotropic distribution of mechanical stresses, zero along and at ±90° to the torque direction, maximum and of opposite sign at ±45°. If a torsion to the right increases the magnetic permeability at +45° it will reduce it at –45°, while a torsion to the left has the inverse effect (see § 6.3 in chap. 12).

A magnetic bridge circuit consists of an excitation arm (P_1, P_2) and a detection arm (S_1, S_2). Flux closure occurs at the shaft, and the detection coils deliver an alternating signal which is proportional to the torsion. The signal cancels out in the absence of a torque, i.e. when the bridge is balanced. Many types of such *torquemeters* exist. The magnetic excitation-detection circuit is separated from the shaft by an airgap, thus it is possible to make measurements on mobile shafts: this type of sensor is interesting for, among others, the automobile industry (fig. 18.9).

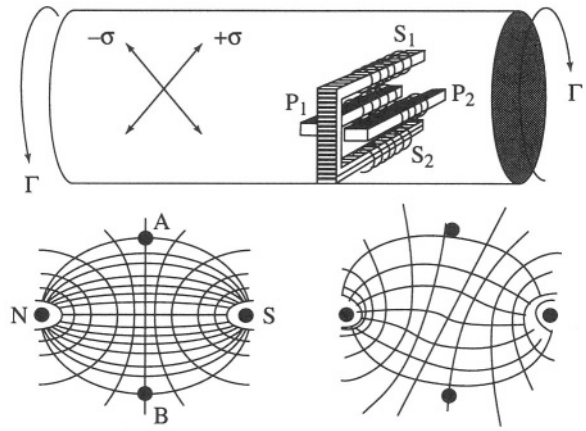

Figure 18.9 - Principle of the "Torductor" torquemeter and schematic diagram of the equipotential lines before and after deformation [14]

If the shaft is non-magnetic, or if the distribution of stresses at the surface of the bar is too inhomogeneous, it is possible to stick Metglas ribbons to the surface which act as the active element of the sensor.

We now mention the multisensor of Tyren and Lord, designed to simultaneously measure the torsion torque and angular velocity of a rotating shaft [15]. This sensor comprises an amorphous ribbon, stuck to the surface of a shaft, which is sensitive to torque related stresses; when its permeability varies, the inductance of a coil, wound around the ribbon and connected in series with a capacitance, is modified. The LC circuit thus established is entirely passive, and turns with the axle to which it is attached. A stationary emitter-detector measures the resonance frequency of the LC circuit: measuring the frequency variation we can calculate the intensity of the torsion torque while the intensity of the received signal, modulated at each turn of the shaft, gives the angular velocity. Moreover the same emitter, working at many different frequencies, can control many sensors located at different points of the rotating part.

3.3. SENSORS BASED ON DIRECT MAGNETOELASTIC EFFECTS

3.3.1. Magnetostrictive magnetometers

The direct Joule magnetostriction effect can be used to detect and measure extremely small magnetic field variations: the US Naval research labs are very active in this area of high resolution magnetometry. Various techniques can be used: e.g. modulation of the optical path in an interferometer in which a bar of Terfenol-D, which is sensitive to the field variations, is inserted; or variation, as a function of the intensity of the magnetic field, of the index of refraction of an optic fibre which is covered with a layer of Metglas [16, 17].

The sensitivity of such devices can reach 10^{-3} to 10^{-4} $A.m^{-1}$.

3.3.2. Position detector

The direct Wiedemann effect has been used to generate a local *shear* which then propagates along a wire or rod. For example, a ring shaped permanent magnet can slide along the outside of a ferromagnetic tube. When a current impulse goes through the tube, a shear occurs at the level of the ring (where the resulting magnetic field becomes helical for a short instant). This deformation pulse then propagates along the tube, and is detected at the tube end. A measure of the transit time allows this device to be used as a *position sensor,* e.g. the Captosonic device commercialised by Equipiel (fig. 18.10).

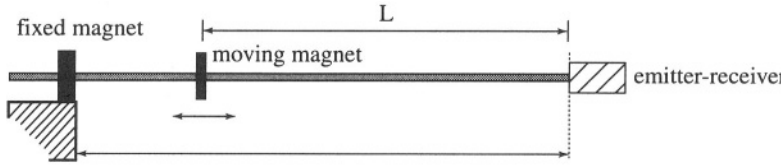

Figure 18.10 - The "Captosonic" position sensor [18]

4. INTEGRATED ACTUATORS AND SENSORS

The development of integrated microsystems has given rise to active research into magnetoelastic effects in thin films.

The aim is to achieve the greatest possible deflection in the smallest magnetic field possible: thus the aim is to find a material which has, at the same time, a strong magnetoelastic coupling coefficient $b^{\gamma,2}$, and as weak as possible an anisotropy field, that is a low magnetic anisotropy and a high magnetization, so as to have a high derivative $\partial b(H)/\partial H$. The most important parameter is thus $b(H)$ (or the coefficient $b^{\gamma,2}$), and not the function $\lambda(H)$ (or the coefficient $\lambda^{\gamma,2}$) as with bulk materials (see § 4.6 of chap. 12).

Studies are still at the exploratory stage, but it already seems that amorphous rare earth-cobalt thin films have much better magnetostrictive characteristics than amorphous thin films of Terfenol, which are based on rare earths and iron. The latter show a notable sperimagnetism (see fig. 4.21), and consequently, a very low magnetization.

Amorphous Tb-Co films have quite a high magnetostriction, but a relatively low magnetization, so that it was proposed to create an artificial structure consisting of alternating layers of Tb-Co and Fe-Co: the Fe-Co alloy is crystallised and has a high magnetization. Provided the alternating layers are not too thick, a strong magnetic coupling may occur between the different Fe-Co layers thus reinforcing the exchange field in the amorphous magnetostrictive layers, and both magnetizations thus rotate together: this multilayered material thus possesses both a notable magnetostriction and a low saturation field.

$Fe_{0.75}Co_{0.25}/Tb_{0.27}Co_{0.73}$ (5.5 nm/4.5 nm) multilayers can have significant values of magnetostriction in weak fields (3.5×10^{-4} deformation in a field of under $80\ kA.m^{-1}$), as can be seen in figure 18.11, where their high performances are compared with those of amorphous $Tb_{0.27}Co_{0.73}$.

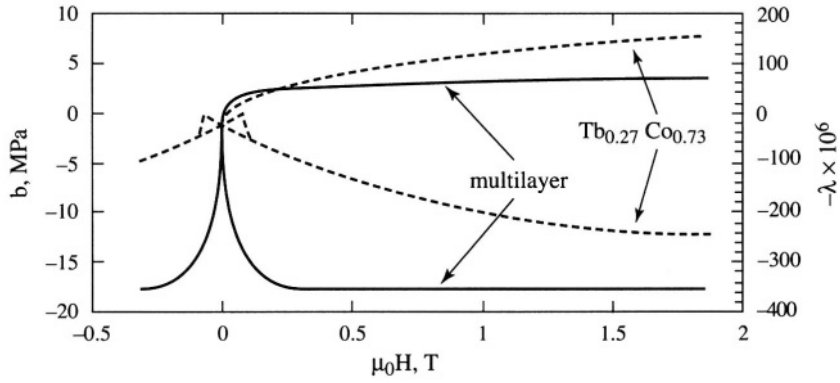

Figure 18.11 - Field variation of the magnetoelastic function b(H) defined by equation (12.23) for two thin films

Comparison between a crystallised thin film of $Tb_{0.27}Co_{0.73}$ and a multilayer of composition $Fe_{0.75}Co_{0.25}/Tb_{0.27}Co_{0.73}$ (4.5 nm/5.5 nm). The right hand scale is the magnetostriction that would be observed for a bulk material with the same magnetoelastic coupling assuming a shear modulus of 50 GPa [19].

Even more spectacular performances were obtained for multilayers of composition $Fe_{0.75}Co_{0.25}/Tb_{0.18}Co_{0.82}$ (6.5 nm/4.5 nm) which have a magnetoelastic coupling coefficient $b^{\gamma,2} = -44.5$ MPa ($\lambda^{\gamma,2} = 890 \times 10^{-6}$), and a derivative, under a field of 2 mT, of $\partial |b^{\gamma,2}| / \mu_0 \partial H = 4{,}800\ MPa.T^{-1}$ [20].

The deformations achieved with such multilayers are now sufficient to plan making micro-actuators, which can be controlled from a distance by simply applying a magnetic field. These devices will find applications in surgery or in medicine (micro-pumps for the controlled delivery of medicine internally, micro-scalpels, etc.), or in electronics, e.g. to make rapid response micro-switches.

A thin film magnetostrictive actuator could work in torsion mode (something which is not possible with piezoelectric materials): this mode lends itself well to a compensation of the thermal derivative [21]; nevertheless, the mechanical realization of such a device remains difficult.

5. CONCLUSIONS AND PERSPECTIVES

Magnetostrictive materials have a bright future in sensor applications, principally because of the possibility to sense the control signal from a distance and without wires, which is not the case for piezo-electric ceramics. For the same reason,

magnetostrictive micro-actuators and micro-sensors are beginning to be used in medical applications, though research in this area is just beginning.
More classical magnetostrictive actuators (motors, sonar devices) must compete with piezoelectric ceramics, which are less expensive, and which are continuously being improved. However, there exists a potential market in space applications where mass reduction is paramount and in very low frequency underwater applications.

EXERCISES

E.1. The forced magnetostriction of an Invar alloy is giant (see § 1.1 of this chapter: $\partial V / V \partial H = 1.2 \times 10^{-10} / A.m^{-1}$). Given the linear thermal expansion coefficient of this alloy between 0°C and 100°C (tab. 18.1), calculate the strength of the magnetic field which is sufficient to produce in a bar of Invar a magnetostrictive expansion equal to the expansion that would result if the bar were heated by 10 degrees from the temperature of melting ice. Deduce the precautions to be taken so that Invar is used under optimum conditions.

E.2. We would like to build a gaussmeter (device for measuring magnetic field strengths) using an optical interferometer to measure the elongation of a bar of Terfenol-D which is 20 cm long and correctly polarised. What will be the maximum displacement in the bar for a magnetic field variation of $1\ A.m^{-1}$? Discuss the range of applications of such a gaussmeter.

E.3. Calculate the theoretical variations (fig. 18.2) in the relative deformation $\lambda_{//} / \lambda_s$ of a bar of Terfenol-D as a function of applied pressure for $H = 100\ kA.m^{-1}$. Suppose that $\lambda_s \approx 10^{-3}$.

E.4. In order to obtain sheets of paper with a constant thickness, a papermaker would like to position, to within a micron, a one ton roller to flatten out the paper paste. Knowing that the movement of the actuators should be $\pm 10\ \mu m$ about the equilibrium position, to take account of the mechanical wear of the moving pieces, propose a magnetostrictive solution to this problem. Data in figure 18.2 and table 18.3 may be useful.

E.5. Is it possible to design a balance based on the principle of figure 18.8 and using Metglas 2605SC as the active element?

SOLUTIONS TO THE EXERCISES

S.1. A magnetic field of $150\ kA.m^{-1}$ would give a *linear deformation* of 6×10^{-6} which is equivalent to a heating by 10°. It is thus advisable to avoid bringing a

powerful magnet near Invar parts if an excellent dimensional stability is to be guaranteed.

S.2. Table 18.3 shows that the best Terfenol-D material (Etrema) can have a magnetostrictivity of $57\times10^{-9}/\mathrm{A.m^{-1}}$. A 20 cm bar is thus elongated by 11.4 nm for a field $1\ \mathrm{A.m^{-1}}$, i.e. $1/50^{\mathrm{th}}$ of a fringe. It is possible to detect $1/1{,}000^{\mathrm{th}}$ of a fringe with a good quality interferometer, thus this type of gaussmeter could detect a static magnetic field of $50\ \mathrm{mA.m^{-1}}$ ($\mu_0 H = 60$ nT).

S.3. The theoretical curve of figure 18.2 could be calculated by minimising the total energy, $E = E_{el} - \mu_0 M_s H \cos\varphi - (3/2)\lambda_s \sigma (\cos^2\varphi - 1/3)$ of a bar subjected to a magnetic field H, and a compressive stress σ, both applied along the length of the bar: $\partial E/\partial\varphi = 0$.

Two solutions exist, $\cos\varphi = -\mu_0 M_s H/3\lambda_s\sigma$, and $\varphi = 0$.

Applying equation (12.20) with $\varphi = \theta$, under zero stress, the demagnetised state being isotropic, $\lambda_0 = 0$, and the application of a field saturates the material ($\varphi = 0$), we thus observe $\lambda_{//} = \lambda_s$. Under weak compressive stress, $P = -\sigma$, the demagnetised state is characterised by $\varphi = \pi/2$, and thus $\lambda_0 = -\lambda_s/2$. Thus there is a discontinuity in the variation of $\lambda - \lambda_0$ as a function of P at P = 0. In the saturated state, $\varphi = 0$, and we thus observe $\lambda_{//} = \lambda_s - \lambda_0 = (3/2)\lambda_s$. Finally, when the stress increases beyond the value for which $\mu_0 M_s H = 3\lambda_s P$, the cosine becomes less than one, and it is the second solution which holds, then:

$$\lambda_{//} = \lambda - \lambda_0 = (3/2)\lambda_s \cos^2\varphi = (3/2)\lambda_s (\mu_0 M_s H/3\lambda_s P)^2 \qquad (18.2)$$

which varies as $1/P^2$. The difference with the experimental curve is explained by the fact that this simple model ignores all anisotropy effects.

S.4. The bearings carrying the roller must rest on 2 actuators which each carry 500 kg, i.e. 5 kN. Figure 18.2 shows that –under a maximum magnetic field of $100\ \mathrm{kA.m^{-1}}$– the maximum magnetostriction is 1.12×10^{-3}, and thus the minimum length of the actuators, h, is $(20/1.12\times10^{-3})\ \mu$m, i.e. 18 mm. A pressure of 20 MPa must be exerted to obtain the desired movement, imposing a cross-section of $S = 2.5\ \mathrm{cm^2}$ for each bar. The necessary volume of terfenol-D is thus $2\times4.5\ \mathrm{cm^3}$. It is possible to change the dimensions, increasing the length and reducing the cross-section, provided that the pressure remains less than the compression limit (700 MPa): for l = 25 mm, P = 35 MPa which gives a cross-section of $1.43\ \mathrm{cm^2}$ and thus a volume of $2\times3.58\ \mathrm{cm^3}$. Finally for l = 44.5 mm, P = 50 MPa the cross-section is $1\ \mathrm{cm^2}$, and the volume of terfenol-D is $2\times4.45\ \mathrm{cm^3}$. Thus the best would be to use two bars of about 25 mm in length and 13.5 mm in diameter, so as to minimise the mass of terfenol-D.

S.5. No, because the magnetostriction of 2605SC is positive, and the sensor in figure 18.8 works only for negative magnetostriction.

REFERENCES

[1] G. BERANGER, F. DUFFAUT, J. MORLET, J.F. TIERS, Les Alliages de Fer et de Nickel (1996) Technique et documentation, Lavoisier, Paris.

[2] Technical document (1994) Imphy SA.

[3] T.G. KOLLIE, *Phys. Rev.* **B16** (1977) 4872.

[4] G.G. WU, X.G. ZHAO, J.H. WANG, J.Y. LI, K.C JIA, W.S. ZHAN, *Appl. Phys. Lett.* **67** (1995) 2005;
X.G. ZHAO, G.G. WU, J.H. WANG, K.C JIA, W.S. ZHAN, *J. Appl. Phys.* **79** (1996) 6225.

[5] T. MORI, T. NAKAMURA, H. ISHIKAWA, *Actuator 98,* VDI-VDE-Technologiezentrum Informationstechnik GmbH (1998) Berlin.

[6] A.E. CLARK, Proc. 3rd Intern. Conf. on New Actuators, VDI-VDE-Technologiezentrum Informationstechnik GmbH (1992), 127, Berlin.

[7] E. DU TRéMOLET DE LACHEISSERIE, Magnetostriction: Theory, and Applications of Magnetoelasticity (1993) C.R.C. Press, Boca Raton, USA.

[8] T. CEDELL, L. SANDLUNG, M. FAHLANDER, Proc. 2nd Intern. Technology Transfer Congress, VDI-VDE-Technologiezentrum Informationstechnik GmbH (1990), 156, Berlin.

[9] V.I. AKSININ, V.V. APOLLONOV, S.A. CHETKIN, V.V. KIJKO, A.S. SAVRANSKI, Proc. 3rd Intern. Conf. on New Actuators, VDI-VDE-Technologiezentrum Informations-technik GmbH (1992), 147, Berlin.

[10] L. KIESEWETTER, Proc. 2nd Intern. Conf. on Giant Magnetostrictive Alloys (1988), C. Tyren Ed., Marbella.

[11] J.M. VRANISH, D.P. NAIK, J.B. RESTORFF, J.P. TETER, *IEEE Trans. Magn.* **27** (1991) 5355.

[12] F. CLAEYSSEN, N. LHERMET, R. LE LETTY, J.C. DEBUS, J.N. DECARPIGNY, B. HAMONIC, G. GROSSO, *Proc. Undersea Defence Technology* **93** (1993) 246, Microwave Exh. and Pub. Ltd. Ed., London.

[13] J. SEEKIRCHER, B. HOFFMANN, *Sensors and Actuators* **A21-A23** (1990) 401.

[14] C.H. TYREN, D.G. LORD, Sensor, European patent PCT/SE90/00444.

[15] H. WINTERHOFF, E.A. HEIDLER, *Technisches Messen* **50** (1983) 461.

[16] J.H. WANDASS, J.S. MURDAY, R.J. COLTON, *Sensors and Actuators* **19** (1989) 211.

[17] M.D. MERMELSTEIN, A. DANDRIDGE, *Appl. Phys. Lett.* **51** (1987) 545.

[18] J.F. PEYRUCAT, *Mesures* **51** (juin 1986) 43.

[19] J. BETZ, Thesis (1997) Université Joseph Fourier, Grenoble, France.

[20] E. QUANDT, A. LUDWIG, J. BETZ, K. MACKAY, D. GIVORD *J. Appl. Phys.* **81** (1997) 5420.

[21] J. BETZ, K. MACKAY, J.C. PEUZIN, B. HALSTRUP, N. LHERMET, *Actuator 96 Conference Proc.* **5** (1996) 283, Axon Technology Consult Gmbh, Bremen, Germany.